

Article

Mechanism of Anti-*Trypanosoma cruzi* Action of Gold(I) Compounds: A Theoretical and Experimental Approach

Javiera Órdenes-Rojas^{1,2}, Paola Risco³, José Ortega-Campos^{1,2}, Germán Barriga-González³ , Ana Liempi² , Ulrike Kemmerling² , Dinorah Gambino⁴ , Lucía Otero⁴, Claudio Olea Azar^{1,*} and Esteban Rodríguez-Arce^{1,4,*} 

¹ Departamento de Química Inorgánica y Analítica, Facultad de Ciencias Químicas y Farmacéuticas, Universidad de Chile, Dr. Carlos Lorca Tobar 964, Casilla 223, Santiago 8380494, Chile; javiera.ordenes@ug.uchile.cl (J.Ó.-R.); jose.ortega.c@uchile.cl (J.O.-C.)

² Instituto de Ciencias Biomédicas, Facultad de Medicina, Universidad de Chile, Av. Independencia 1027, Santiago 8380453, Chile; anitavet@gmail.com (A.L.); ukemmerling@uchile.cl (U.K.)

³ Laboratorio MACEDONIA, Departamento de Química, Universidad Metropolitana de Ciencias de la Educación, Av. José Pedro Alessandri 774, Santiago 7760197, Chile; german.barriga@umce.cl (G.B.-G.)

⁴ Área Química Inorgánica, Facultad de Química, Universidad de la República, Gral. Flores 2124, Montevideo 11800, Uruguay; dgambino@fq.edu.uy (D.G.); luotero@fq.edu.uy (L.O.)

* Correspondence: colea@uchile.cl (C.O.A.); esteban.rodriguez.arce@gmail.com (E.R.-A.)

Abstract: In the search for a more effective chemotherapy for the treatment of Chagas' disease, caused by *Trypanosoma cruzi* parasite, the use of gold compounds may be a promising approach. In this work, four gold(I) compounds [AuCl(HL)], (HL = bioactive 5-nitrofuryl containing thiosemicarbazones) were studied. The compounds were theoretically characterized, showing identical chemical structures with the metal ion located in a linear coordination environment and the thiosemicarbazones acting as monodentate ligands. Cyclic voltammetry and Electron Spin Resonance (ESR) studies demonstrated that the complexes could generate the nitro anion radical (NO₂⁻) by reduction of the nitro moiety. The compounds were evaluated in vitro on the trypomastigote form of *T. cruzi* and human cells of endothelial morphology. The gold compounds studied showed activity in the micromolar range against *T. cruzi*. The most active compounds (IC₅₀ of around 10 μM) showed an enhancement of the antiparasitic activity compared with their respective bioactive ligands and moderate selectivity. To get insight into the anti-chagasic mechanism of action, the intracellular free radical production capacity of the gold compounds was assessed by ESR and fluorescence measurements. DMPO (5,5-dimethyl-1-pyrroline-N-oxide) spin adducts related to the bioreduction of the complexes and redox cycling processes were characterized. The potential oxidative stress mechanism against *T. cruzi* was confirmed.

Keywords: gold compounds; thiosemicarbazones; *Trypanosoma cruzi*; free radicals



Citation: Órdenes-Rojas, J.; Risco, P.; Ortega-Campos, J.; Barriga-González, G.; Liempi, A.; Kemmerling, U.; Gambino, D.; Otero, L.; Olea Azar, C.; Rodríguez-Arce, E. Mechanism of Anti-*Trypanosoma cruzi* Action of Gold(I) Compounds: A Theoretical and Experimental Approach. *Inorganics* **2024**, *12*, 133. <https://doi.org/10.3390/inorganics12050133>

Academic Editor: Bruno Therrien

Received: 6 April 2024

Revised: 28 April 2024

Accepted: 30 April 2024

Published: 3 May 2024



Copyright: © 2024 by the authors. Licensee MDPI, Basel, Switzerland. This article is an open access article distributed under the terms and conditions of the Creative Commons Attribution (CC BY) license (<https://creativecommons.org/licenses/by/4.0/>).

1. Introduction

Neglected Tropical Diseases (NTDs) are a diverse group of 20 conditions mainly prevalent in tropical areas worldwide. These illnesses affect impoverished communities and cause devastating health, social, and economic consequences to more than one billion people [1]. The epidemiology of NTDs is complex and the pharmaceutical industry does not invest in drug research to combat NTDs because of the low associated revenue, which makes their public health control challenging. Among them, American Trypanosomiasis, or Chagas' disease, caused by the protozoan parasite *Trypanosoma cruzi* (*T. cruzi*), affects around 7 million people worldwide, mostly in Latin America [2]. In the endemic zones, the *T. cruzi* parasites are mainly transmitted to mammalian hosts by infected blood-sucking insects. In addition, other modes of transmission have spread the disease to non-endemic regions, such as blood transfusion, organ transplants, and congenital transmission.

The currently available chemotherapy includes drugs developed more than 50 years ago, Nifurtimox and Benznidazol. These drugs are efficient only in the acute phase of the disease, but they are not effective in clinical treatment during the chronic phase. Moreover, these clinically approved drugs present toxicity, require long treatments, and often the parasites develop resistance to them [3]. Although some synthetic and natural compounds have been tested against *T. cruzi*, few have been successfully processed through clinical trials [4–6]. In this context, the development of new drugs is urgently needed for the effective treatment of Chagas' disease.

Medicinal Inorganic Chemistry has proven to be a promising approach in the search for new therapeutic agents against Chagas' disease. Prospective metal-based drugs, which include different metal ion that acts through diverse mechanisms of action, have been identified [7–9]. In this respect, our main design strategy has been to develop metal compounds with known bioactive molecules as ligands, in particular the bioactive 5-nitrofuryl containing thiosemicarbazones (HL, Figure 1). These molecules contain the same 5-nitrofuran pharmacophore as the drug Nifurtimox. The 5-nitrofuryl-containing thiosemicarbazones have shown good activities in vitro against *T. cruzi*; however, they also showed cytotoxicity against mammalian cells [10]. The main mechanism of action of these bioactive molecules is based on the bioreduction of the nitro group to a nitro anion radical, generating toxic reactive oxygen species (ROS) against *T. cruzi* [10].

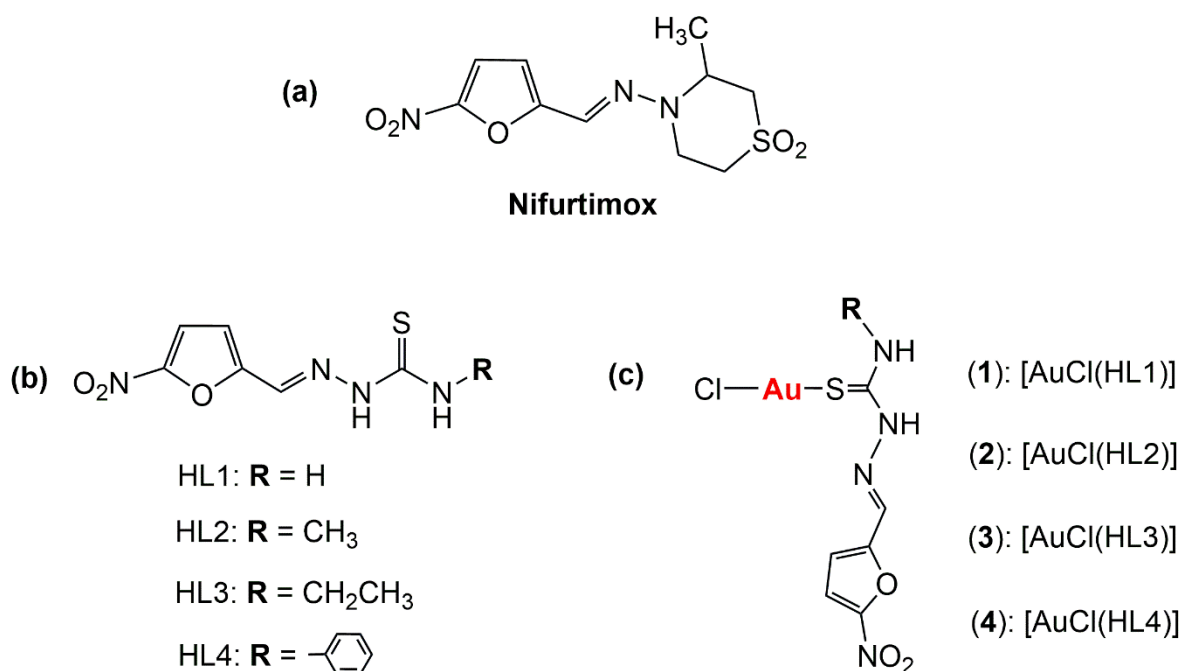


Figure 1. Chemical structure of (a) Nifurtimox, (b) 5-nitrofuryl-containing thiosemicarbazone ligands, and (c) [AuCl(HL)] compounds.

In order to improve the pharmacological properties of these bioactive organic molecules, 72 classical and organometallic compounds had been previously synthesized. These metal compounds included Pt(II), Pd(II), Ru(II), Ru(III) and Re(I) metal centers, and different co-ligands to modulate biologically relevant physicochemical properties [8,11]. Among them, the complexes that included Pt(II) metal center and lipophilic co-ligands such as dppf (1,1'-bis(diphenylphosphino)ferrocene) have been the most active complexes against *T. cruzi* [12].

On the other hand, gold compounds currently have several medicinal applications. They have long been used in the treatment of rheumatoid arthritis and tuberculosis [13], and some gold complexes are in clinical trials as potential anticancer agents [14]. However, a small number of gold(I) compounds have been evaluated as potential metal-based drugs

against *T. cruzi*. These compounds have included bioactive ligands such as Clotrimazole (CTZ) [15] and pyridine-2-thiol *N*-oxide (mpo) [16]. In particular, the trypanocidal activity of the Au(I)-mpo compound was associated with the inhibition of NADH fumarate reductase activity, a kinetoplastid parasite-specific enzyme absent in the host [16]. Gold(I) ion is a soft Lewis acid and has a high affinity for thiol groups present in biomolecules. It has been confirmed that the gold compounds could act as cysteine protease inhibitors, which gives them potential pharmaceutical applications [17]. Gold(I) compounds including thiosemicarbazone-derived ligands with activity against *T. cruzi* have still not been reported.

Recently, gold(I) compounds that include 5-nitrofuryl-containing thiosemicarbazones were synthesized and fully characterized [18]. The [AuCl(HL)] complexes (Figure 1) were evaluated as potential anticancer agents in a panel of human cancer cells. The complexes demonstrated high activity and selectivity, and their main mechanism of action was related to the capacity of the compounds to accumulate in the cancer cell nuclei and interact with DNA, which caused subsequent cancer cell death via apoptosis [18].

Parasites and neoplastic cells have common features. For example, they present some similar metabolic processes, and both have common antigens and enzymes [19–21]. The presence of common targets favors the effectiveness of certain molecules as both anticancer drugs and antiprotozoal agents. Several drugs that have proved active as antiparasitic agents have also been efficacious preclinically as anticancer agents [22,23].

Due to the promising anticancer activity reported for [AuCl(HL)] compounds, we propose that these complexes might also be useful as potential anti-*T. cruzi* agents. In this work, we theoretically characterized the neutral and radical chemical structure of the gold(I) compounds and evaluated the in vitro activity against *Trypanosoma cruzi*. In addition, we studied the probable anti-chagasic mechanism of action of the compounds related to ROS generation.

2. Results and Discussion

2.1. Theoretical Calculations

As previously mentioned, the [AuCl(HL)] (1–4) compounds had been recently synthesized and fully characterized in solid state and solution [18]. However, no crystallographic data of the monomeric structures had been obtained due to the low solution stability reported for these complexes. In this work, we have calculated theoretically the chemical structure of the gold compounds to evaluate their electronic properties and spin density distribution for correlating them with the experimental ESR spectra.

After performing a conformational search, the minimum energy conformation was obtained and then, geometry optimization using ORCA was carried out. In all cases, the theoretical calculations were performed using DMSO as the solvent to simulate the experimental conditions (see below). The geometry optimization results showed that all the compounds would have an identical chemical structure, with the metal ion located in a linear coordination environment and the thiosemicarbazone acting as monodentate ligands in *Z*-conformation (Figure 2).

Natural Bond Orbital (NBO) Analysis

Considering that the probable mechanism of action of the [AuCl(HL)] compounds could be related to the generation of the nitro anion radical, Natural Bond Orbital (NBO) studies were performed. A second-order perturbation analysis was developed to identify the electronic delocalization for the four gold compounds. These studies allowed us to analyze the effect of gold(I) and the different R substituents of the thiosemicarbazone on the electronic delocalization of the nitro anion radical. Therefore, all studies were performed on the molecule in the radical anion state. Table 1 shows, as an example, the results obtained for compound 1, and Tables S1–S3 summarize the results for the rest of the compounds. Figures S1–S4 show the NBO-selected bonds for the four gold complexes.

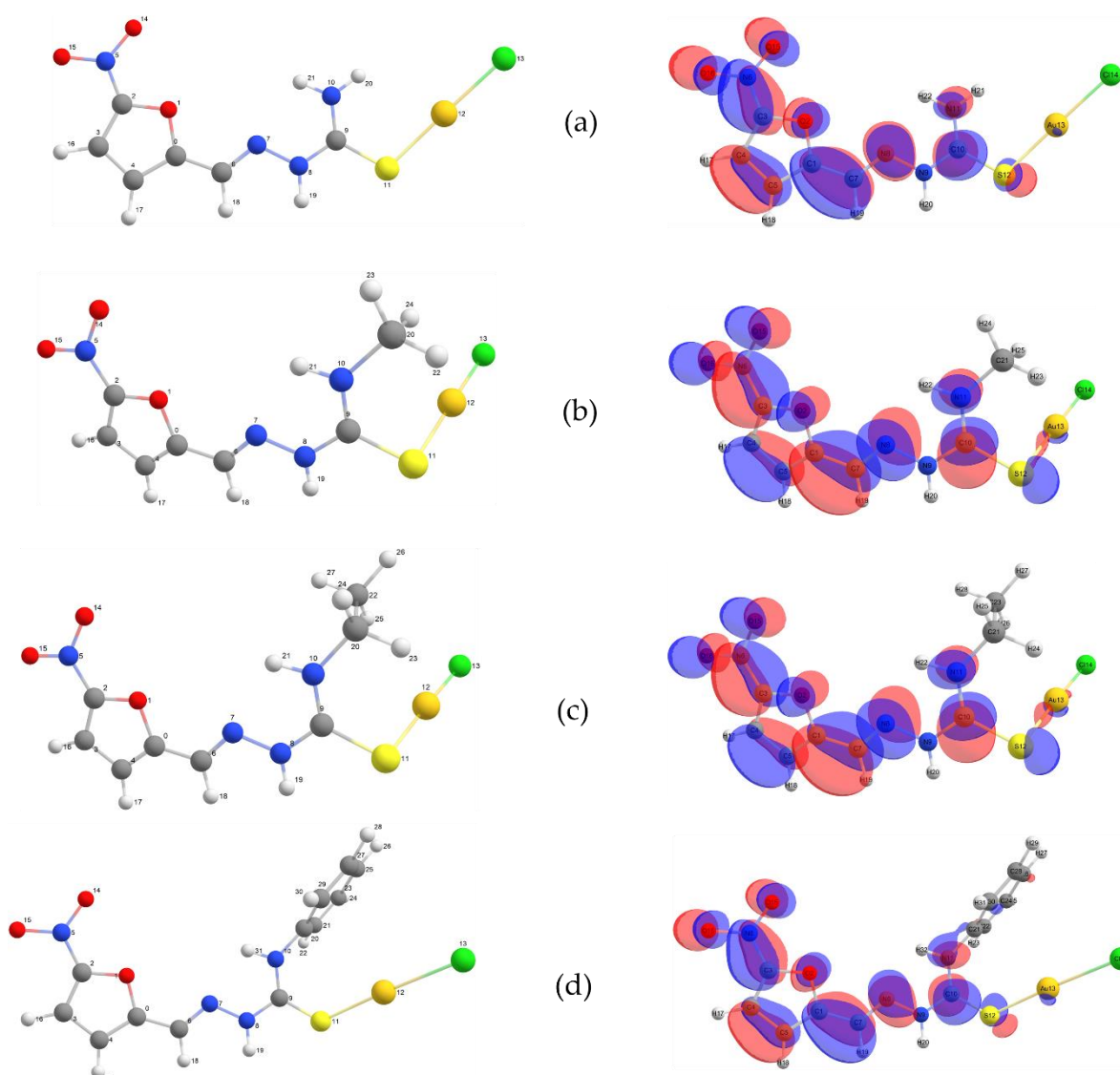
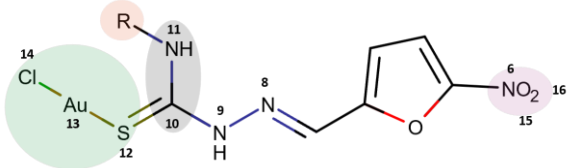


Figure 2. Optimized structures (**left**) and LUMO calculated (**right**) for (a) [AuCl(HL1)] (**1**), (b) [AuCl(HL2)] (**2**), (c) [AuCl(HL3)] (**3**), and (d) [AuCl(HL4)] (**4**) compounds. Colors correspond to the following atoms: oxygen (red), nitrogen (blue), carbon (gray), hydrogen (white), sulfur (yellow), gold (orange), and chloro (green).

The non-bonding electron pair of N9 stabilized the antibonding orbital formed by C10-N11 atoms for the alpha wave function. The sulfur atom stabilized the same bond with one of its pairs of unshared electrons but at a lower energy value (see Table 1). Thus, the Au-S bond stabilization was achieved by an electron pair from the chlorine atom. The beta electrons showed higher stabilization energy due to an electron pair from N6 bonding with the oxygen atoms attached to form the nitro group. The C10-N11 antibonding orbital was also stabilized by a sulfur atom at a similar energy value. Similar behavior was observed for compounds **2**, **3**, and **4** after replacing one of the hydrogen atoms bonded to N11 for the methyl, ethyl, and phenyl groups, respectively. However, for compound **4**, the unshared electron pair from the chlorine atom that stabilizes the bond S-Au in all previous compounds was not observed.

Table 1. Natural Bond Orbital (NBO) results for [AuCl(HL1)] (1) compound.


Spin	Donor (L) NBO ¹	Acceptor (NL) NBO ²	E(2) ³ kcal/mol
α	32. LP (1) N 11	93. BD*(1) C 10–N 9	73.13
α	34. LP (2) S 12	93. BD*(1) C 10–N 9	33.07
α	43. LP (4) Cl 14	99. BD*(1) S 12–Au 13	75.17
β	30. LP (1) N 6	99. BD*(1) O 15–O 16	1075.57
β	32. LP (1) N 9	93. BD*(1) C 10–N 11	68.87
β	34. LP (2) S 12	93. BD*(1) C 10–N 11	35.94
β	43. LP (4) Cl 14	98. BD*(1) S 12–Au 13	75.13

¹ L corresponds to the “Lewis orbital” type with an occupation number near two. ² NL corresponds to the “non-Lewis orbital” type with an occupation number near zero. ³ When the non-Lewis orbital exhibits higher E(2) values, this means significant delocalization effects. LP is a lone pair of electrons. BD* is an anti-bonding natural orbital. The numbers on the left of each atom correspond to the respective NBO orbitals.

The gold(I) metal center did not exhibit effects on the electronic density of the nitro anion radical. Meanwhile, the different substituents of the amine terminal group showed a small decrease in stabilization over the C–N bond from the imino group. This bond showed an increase of the energy for the alpha electrons of around 3 kcal/mol when increasing the size of the substituent group. An inverse tendency was exhibited by the compounds for the beta electrons, showing lower energy changes at around 1 kcal/mol.

Finally, a high value of E(2) in the nitro group region for all compounds was observed. These values indicate a large zone of electronic delocalization centered on the nitro anion radical. Compound **1** showed higher E(2) values than the rest of the compounds. These values decreased gradually with the increase in the aliphatic chain length of the substituent groups in the thiosemicarbazone ligands.

2.2. Cyclic Voltammetry

The electrochemical behavior of the [AuCl(HL)] compounds was studied at room temperature by cyclic voltammetry in DMSO solutions. The compounds were evaluated in the negative potential zone using a hanging drop mercury electrode. Figure 3 shows the voltammograms obtained for **2** and the HL2 ligand. Selected electrochemical data for all complexes are shown in Table 2.

The compounds showed three ligand-centered electrochemical processes. These redox couples have been previously reported for the 5-nitrofuryl-containing thiosemicarbazone ligands (HL) and their metal compounds [24,25]. The redox couple I could be assigned to the quasi reversible self-protonation process of the HL ligands [24,25].

The second electrochemical process (couple II) at around -0.9 V (vs. Ag/AgCl) corresponds to a quasi-reversible reduction by one electron of the nitro group to a nitro anion radical ($\text{NO}_2^{\cdot-}$). A minimum variation in the reduction potential values of the thiosemicarbazone ligands upon gold(I) coordination was observed. This behavior agrees with the theoretical NBO calculations, which indicated that the gold(I) center does not generate a significant effect on the reactivity of the nitro group. The electrochemical behavior of Nifurtimox, the anti-chagasic reference drug, was evaluated under the same

experimental conditions. Nifurtimox also showed this reversible reduction process to generate the nitro anion radical, which agrees with their principal mechanism of action. For the gold(I) compounds, this couple was observed at less negative potentials. This change could be biologically relevant since it would further favor the generation of ROS in the *T. cruzi* parasites in comparison to Nifurtimox. Therefore, this bioreduction process could be one principal mechanism involved in the biological action of the [AuCl(HL)] compounds against *Trypanosoma cruzi*, as it is for the free ligands [10].

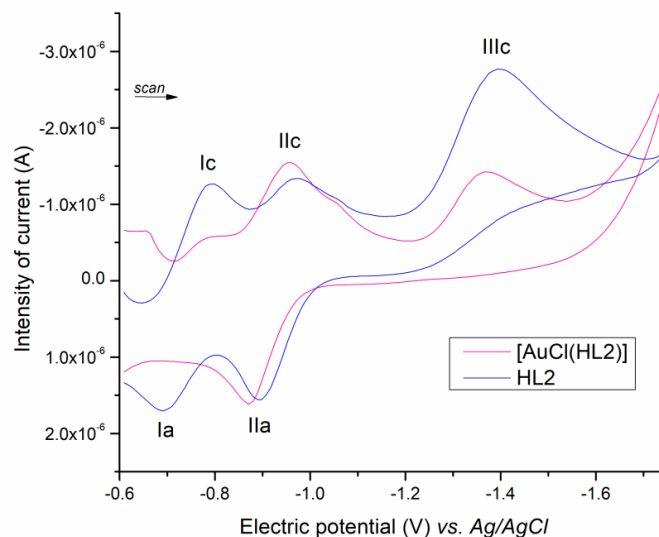


Figure 3. Cyclic voltammograms of [AuCl(HL2)] (2) compound and the HL2 ligand measured in the cathodic direction at $1.0 \text{ V}\cdot\text{s}^{-1}$. Experimental conditions: Samples 1 mM in DMSO solution, hanging drop mercury working electrode, Pt wire auxiliary electrode, Ag/AgCl reference electrode, and supporting electrolyte $0.1 \text{ mol}\cdot\text{L}^{-1}$ TBAP.

Table 2. Selected potential values (Volts) for [AuCl(HL)] compounds and Nifurtimox in 1mM DMSO solutions at a scan rate of $1.0 \text{ V}\cdot\text{s}^{-1}$. The values in parentheses correspond to the potentials of the free ligands reported in reference [12].

Compound	Couple I		Couple II		Couple III
	E_{pc}^1	E_{pa}^2	E_{pc}^1	E_p^2	E_{pc}
[AuCl(HL1)]	−0.80	-	−0.96 (−0.92)	−0.89 (−0.80)	−1.38
[AuCl(HL2)]	−0.80	−0.73	−0.95 (−0.98)	−0.89 (−0.85)	−1.39
[AuCl(HL3)]	−0.79	−0.72	−0.93 (−0.95)	−0.87 (−0.84)	−1.35
[AuCl(HL4)]	−0.75	−0.74	−0.92 (−0.92)	−0.86 (−0.81)	−1.38
Nifurtimox	-	-	−1.18	−1.12	-

¹ E_{pc} : cathodic peak potential. ² E_{pa} : anodic peak potential.

Previous cyclic voltammetry studies had demonstrated that the bidentate coordination of 5-nitrofuryl thiosemicarbazone to different metal ions leads to a displacement toward less negative potential values of the nitro group/nitro anion radical couple [12]. To analyze the effect of the gold center over the reduction potential of the nitro group of the HL1–HL4 ligands, these results were compared with metal complexes chemically related, such as [PdCl₂(HL)], [PtCl₂(HL)], and [RuCl₂(HL)₂] [24,26,27]. Although no regular trend in reduction potential was observed in complexes that include chloride as co-ligands like those reported here, it is possible to observe that the monodentate coordination to gold(I) ion did not generate a significant change in the reduction potential in comparison with the effect generated by the other metal ions. The shifts toward less negative potential values have been only observed in complexes that include more lipophilic co-ligands [12].

Finally, towards more negative potential values all complexes showed an irreversible reduction process (couple III) that was assigned to the further reduction of the nitro group to the hydroxylamine [25].

2.3. Electron Spin Resonance

The nitro anion radical generated for the $[\text{AuCl}(\text{HL})]$ compounds was characterized and studied by Electron Spin Resonance (ESR). The radicals were prepared in situ in the cavity of the ESR spectrometer by electrochemical reduction in DMSO solutions, applying a potential corresponding to couple II obtained from the voltammetry studies. All gold(I) compounds formed stable paramagnetic intermediates at that first reduction step according to the proposed electrochemical characterization.

The global behavior of the $[\text{AuCl}(\text{HL})]$ complexes is exemplified by the ESR spectrum of compound **1**. Figure 4 summarizes the atoms' numbering system used for ESR signals assignment.

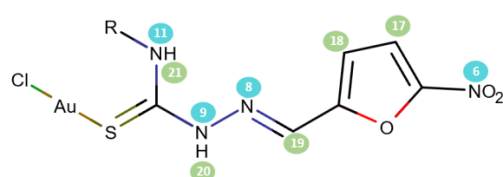


Figure 4. Chemical structure of $[\text{AuCl}(\text{HL})]$ compounds, which includes the hydrogen (green) and nitrogen (light blue) atoms' numbering system used for ESR signal assignment.

After generating the radical species in situ, a spectrum was recorded to determine the hyperfine coupling constants by simulation. Figure 5 shows the spin density calculated for compound **1**, the experimental ESR spectrum, and the simulation of the same spectrum WINEPR-SimFonia 1.25 software. Table 3 summarizes the most relevant hyperfine coupling constant values obtained from WINEPR-SimFonia and the most relevant spin densities calculated by ORCA. Figures S5–S7 show the spin density calculated for compounds **2**, **3**, and **4**, and Table S4 summarizes the complete table of spin densities calculated for all of these compounds.

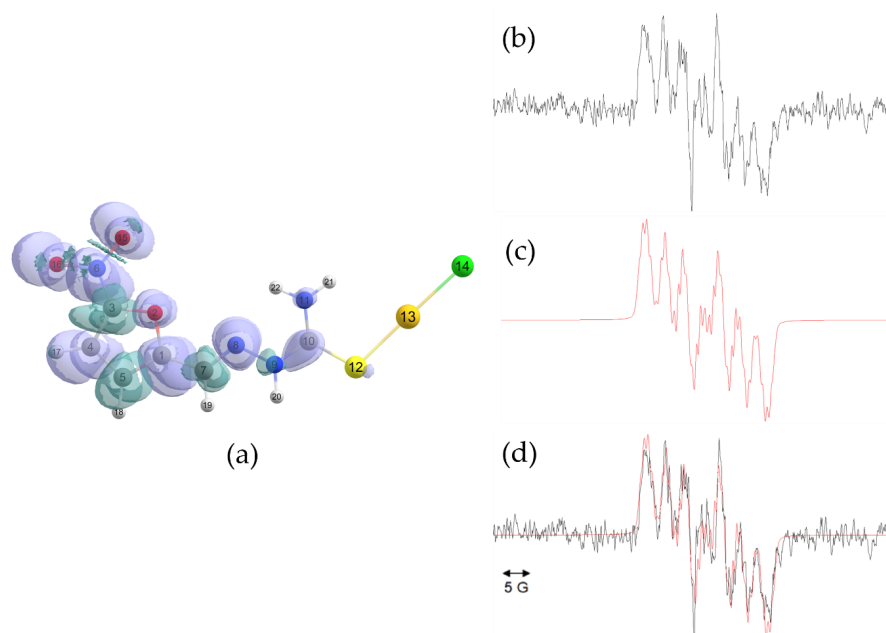


Figure 5. (a) Spin density calculated for $[\text{AuCl}(\text{HL1})]$ (**1**) compound, (b) experimental ESR spectrum recorded between 3430 and 3505 G, (c) simulated spectrum, and (d) overlay of experimental and simulated spectra.

Table 3. Spin density calculated by ORCA and hyperfine splitting constants (a, (G)) determined by WINEPR-SimFonia 1.25 software, for [AuCl(HL)] compounds studied by ESR performing in situ electrochemical generation, with a precision of 0.05 G.

	[AuCl(HL1)]		[AuCl(HL2)]		[AuCl(HL3)]		[AuCl(HL4)]	
	Spin Density	a (G)						
N6	0.202404	8.55	0.199949	9.16	0.200306	9.05	0.196242	8.20
H17	0.000468	5.20	0.000456	5.42	0.000462	5.43	0.00043	5.10
H18	−0.000346	3.28	−0.000343	3.35	−0.000348	3.30	−0.000338	3.40
H19	−0.000119	0.83	−0.000103	0.53	−0.000107	0.96	−0.000087	0.90
N8	0.149215	1.09	0.15112	1.07	0.150759	1.05	0.152195	1.07
N9	0.003226	0.88	0.002067	0.98	0.002081	0.94	0.000466	0.90
H20	−0.000051	0.67	−0.000031	0.46	−0.000034	0.80	−0.000061	0.90
N11	0.00880	-	0.012168	-	0.012004	-	0.00945	-
H21	0.000103	-	−0.000003	-	−0.000012	-	0.000026	-

All compounds present a simulated spectrum with a hyperfine pattern of three triplets assigned to the effect caused by the nitrogen atoms N6 (nitro), N8, and N9 of the thiosemicarbazone, and four doublets assigned to the effect caused by the hydrogens H17 and H18 (furan ring) and H19 and H20 (thiosemicarbazone). The hyperfine coupling constants recorded indicate the existence of a greater delocalization of the unpaired electron fundamentally in the N6 nitrogen of the nitro group of the furan ring. The hyperfine pattern and the determined coupling constants of the complexes have similarities with the hyperfine pattern described for the free ligands [25]. In particular, the hyperfine coupling constants determined for the nitrogen atom N6 (nitro) in the gold(I) compounds were similar to the values reported for [PdCl₂(HL)], and both were higher than the values reported for [PtCl₂(HL)] and [RuCl₂(HL)₂] complexes [24,26,27]. These results suggest that in the [AuCl(HL)] compounds, the electron is preferably more localized in the nitro group than in the rest of the molecule.

In addition, the spin densities and ESR properties on the radical forms of the gold(I) complexes were determined. All analyses were performed using DMSO as the solvent to simulate the experimental conditions. The analysis of the ESR spectrum using a simulation process confirmed the stabilities of the radical species due to the delocalization of the unpaired electron. The isosurfaces obtained for all compounds demonstrate that the spin densities extend throughout the thiosemicarbazone ligand, which is minimally impacted by the presence of the metal ion (see Figure 5 and Figures S5–S7). The subsequent examination of substituents for the terminal amine group showed that H, methyl, ethyl, and phenyl do not have a significant structural impact compared to the parental compound.

2.4. Lipophilicity

Lipophilicity is an important physicochemical property to understand the biological behavior of prospective drugs, such as transmembrane transport and interaction with biological receptors. Thus, its correlation with biological activity is usually a relevant characteristic to be studied.

It has been previously determined that the [AuCl(HL)] compounds present partition coefficient (log P) values between −0.31 to 0.26 [18]. In this work, the lipophilicity was experimentally determined using reversed-phase TLC. This method allows us to determine and compare under the same experimental conditions the lipophilicity of the gold compounds, the free thiosemicarbazone ligands, and Nifurtimox. The stationary phase (silica gel 60 RP-18 F254s) may be considered to simulate membrane lipids or biological receptors, and the mobile phase (DMSO:PBS (80:20 v/v)) resembles the aqueous medium. The com-

position of the mobile phase was tuned up to allow differentiating the gold compounds, the free ligands, and Nifurtimox according to their lipophilicity.

As expected, the lipophilicity of the thiosemicarbazone ligands increased when the substituent group changed from hydrogen to a phenyl group. A small increase in the lipophilicity of the thiosemicarbazone ligands upon gold(I) center coordination was observed, except in the compound with phenyl substituent (Table 4). The R_M values were lower than those reported for chemically related ruthenium(II) compounds, which suggests that the gold(I) ion does not generate a significant increase in the lipophilicity of 5-nitrofuryl-containing thiosemicarbazones ligands [26]. Compound 2 showed a lipophilicity like Nifurtimox with R_M values close to zero.

Table 4. In vitro activity (measured as the IC_{50} value, the half inhibitory concentration) against *T. cruzi* trypomastigotes (Dm28c), cytotoxicity on EA.hy926 human cells of endothelial morphology and selectivity index (SI) values of [AuCl(HL)] compounds, HL1–HL4 ligands, and Nifurtimox (included for comparison). R_M values (lipophilicity) of the complexes, and the corresponding free ligands and Nifurtimox, determined by reversed-phase TLC using DMSO:PBS (80:20 v/v) as the mobile phase, are also depicted.

Compound	<i>T. cruzi</i> $IC_{50}/\mu M$	EA.hy926 $IC_{50}/\mu M$	SI ¹	R_M ³
[AuCl(HL1)] (1)	24.5 ± 1.4	108.2 ± 6.6	4	−0.22
HL1	9.8 ± 1.5 ²	>100 ²	>10	−0.31
[AuCl(HL2)] (2)	10.3 ± 1.0	94.0 ± 1.7	9	−0.01
HL2	17.4 ± 1.9 ²	>100 ²	>6	−0.04
[AuCl(HL3)] (3)	9.9 ± 1.9	46.7 ± 0.7	5	0.13
HL3	18.5 ± 1.7 ²	>100 ²	>5	0.12
[AuCl(HL4)] (4)	49.1 ± 7.3	78.4 ± 2.1	2	0.17
HL4	22.7 ± 1.6 ²	>100 ²	>4	0.29
Nifurtimox	10.0 ± 0.4	>200	>20	0.02

¹ IC_{50} EA.hy926/ IC_{50} *T. cruzi*. ² From reference [12]. ³ $R_M = \log_{10}[(1/R_f)-1]$.

2.5. Biological Studies: Anti-Trypanosoma Cruzi Activity and Cytotoxicity on Mammalian Cells Models

The cytotoxicity of [AuCl(HL)] compounds 1–4 was evaluated in vitro on *T. cruzi* trypomastigotes (Dm28c), as well as human cells of endothelial morphology (EA.hy926). Table 4 shows the cell viability values determined as the ability of the compounds to inhibit cell viability after 24 h incubation using the MTT method.

The four [AuCl(HL)] compounds were active against *T. cruzi* parasites, displaying IC_{50} values in the low micromolar range. Compounds 2 and 3 were the most active compounds, and both showed an enhancement in antiparasitic activity compared with their respective thiosemicarbazone ligands. In addition, compounds 2 and 3 showed similar antiparasitic activity to the reference drug, Nifurtimox. To analyze the effect of the gold(I) on the biological activity of the thiosemicarbazone ligands, it could be observed that this metal ion generated an increase in the biological activity of the HL2 and HL3 ligands, higher than that observed for the complexes with similar chemical structure that include Pd(II), Pt(II), or Ru(II) metal centers [24,26,27].

The specificity of the anti-trypanosomal activity of the compounds was evaluated by analyzing their cytotoxicity against human-derived morphologically endothelial cells (EA.hy926). Complex 2 was the most selective gold compound against *Trypanosoma cruzi*.

Anticancer activity studies recently reported for the [AuCl(HL)] compounds confirmed that the stability in solution and biological media is directly related to the biological activity of the complexes. These studies showed that the compounds evolve in solution to cationic monometallic species ([Au(HL)(DMSO)]⁺ or [Au(HL)]⁺) and/or to neutral dimeric compounds, [[Au(HL)]₂], which always contain the thiosemicarbazone ligands. Compound 2 was the most stable in DMSO and DMSO/culture medium solution for over a week or

72 h, respectively, and was the most cytotoxic and selective compound against different cancer cell lines [18]. In the present work, **2** and **3** were the most active compounds, and particularly compound **2** was also the most selective against *T. cruzi*. Therefore, a quite good correlation between the antineoplastic and antiparasitic effects of the [AuCl(HL)] compounds was identified. As previously mentioned, some antiparasitic agents have shown high effectiveness as potential anticancer drugs [22,23]. Therefore, this relationship of the biological activity of the [AuCl(HL)] compounds could be a good approach for developing prospective gold-based drugs.

Conversely, no clear correlation between the lipophilicity of the compounds and their antiparasitic activity could be identified. However, it was observed that compound **2**, one of the most active and selective gold compounds, exhibited biological activity and lipophilicity similar to those of Nifurtimox. This gold compound also showed the highest hyperfine coupling constant values ($a = 9.16$ G) for the nitrogen atom of the nitro group (see Table 3); hence, their ROS generation ability could be related to their high activity against *T. cruzi*. Based on these results, and as shown in Figure S8, it could be suggested that a high localization of the electron on the nitro group and lipophilicity close to the Nifurtimox could favor the activity and selectivity of the [AuCl(HL)] compounds against *Trypanosoma cruzi* parasites.

2.6. Insights into the Mechanism of Action: Production of Free Radical Species and Reactive Oxygen Species on *Trypanosoma cruzi*

Intracellular bioreduction and consecutive ROS generation is the principal anti-trypanosomal mechanism of action of the 5-nitrofuryl-containing thiosemicarbazone bioactive ligands [10]. This mechanism of action is also maintained by metal compounds that include these thiosemicarbazone ligands [24,26,27]. As stated above, the first step of the mechanism involves the nitro anion radical generation by bioreduction of the nitrofuran moiety. The electrochemical and ESR studies suggest that the four gold(I) complexes would have the ability to generate the $\text{NO}_2^{\cdot-}$ radical. To assess the ROS production capacity in the biological medium of **1–4**, the compounds were incubated with *T. cruzi* parasites (trypomastigotes, Dm28 strain) and then studied by ESR experiments. DMPO was added as a spin-trapping agent to detect radical species of short half-time lives. The global behavior of the gold compounds is exemplified by the ESR spectrum of [AuCl(HL2)], displayed in Figure 6.

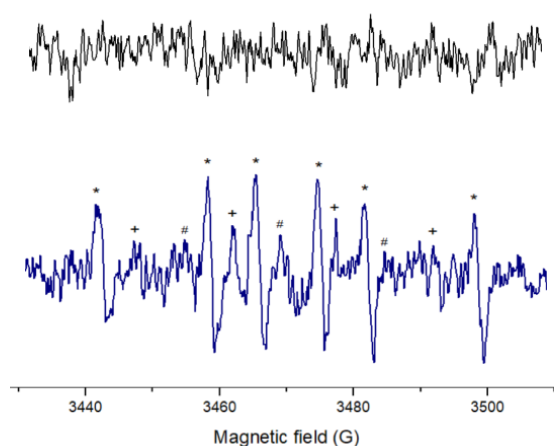


Figure 6. ESR spectra obtained after 15 min incubation of [AuCl(HL2)] (**2**) compound (1 mM) with *T. cruzi* trypomastigotes (Dm28c strain, final protein concentration 4–8 mg/mL), NADPH (1 mM), and DMPO (100 mM). Above: Negative control. Below: [AuCl(HL2)] compound. (*) characteristic signals of DMPO-CH₃ spin adduct. (+) characteristic signals of DMPO-OH spin adduct. (#) DMPOX or DMPO-OH oxidation signals.

ESR spectra of the four [AuCl(HL)] compounds showed a similar thirteen-line pattern, whose signals correspond to three different DMPO spin adducts. One of them corresponds to a six-line pattern (marked with *, Figure 6) related to the trapping of a carbon-centered radical by DMPO ($a_N = 16.3$ G and $a_H = 23.5$ G), associated with the methyl radical generated by the presence of DMSO as a vehicle [28]. The second group of signals (+, Figure 6) consisting of a four-line pattern, corresponds to the DMPO-OH adduct [28]. Intracellular hydroxyl radical species would arise due to the redox cycling process that involves the reduction of the nitro group. The last three-line pattern (#, Figure 6) could be related to the oxidation of the spin trap and/or the rapid decomposition of DMPO-OH adduct (DMPOX) [28].

In addition, the intracellular ROS generation on *T. cruzi* (trypomastigotes, Dm28c) produced by [AuCl(HL)] compounds was quantified in vitro using a 2',7'-dichlorofluorescein (DCF) probe (Figure 7). The four complexes showed the ability to cross the cell membrane, generating an increase in the ratio of fluorescence areas related to the negative control. Moreover, all complexes generated an increase in intracellular ROS in comparison with the reference drug, Nifurtimox. Complex 3 was the compound that generated the greatest amount of intracellular ROS and it was notably one of the most active gold compounds against *T. cruzi*. One-way analysis of variance (ANOVA) was performed with subsequent Tukey's multiple comparisons test to show that only the production of cytosolic ROS produced by compound 3, versus the other compounds, is statistically significant (Figure S9). Based on these results, we could suggest that the antiparasitic activity of the [AuCl(HL)] compounds could be related to their ROS generation ability.

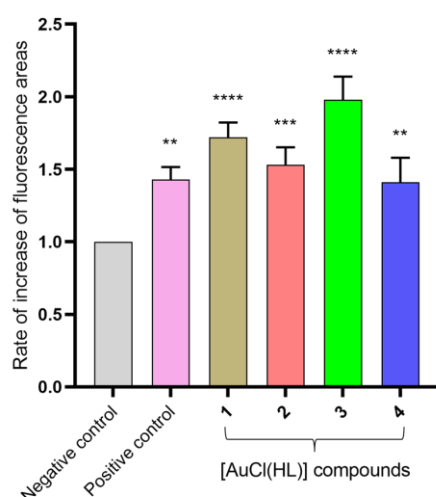


Figure 7. Rate of increase in areas of fluorescence spectra relative to the negative control having a value of 1. Negative control corresponds to parasites without treatment, positive control corresponds to parasites treated with 10 μ M Nifurtimox, and 1–4 corresponds to parasites treated with each gold compound to 10 μ M concentration. For each treatment, one-way analysis of variance (ANOVA) compared to negative control rate was performed with subsequent Dunnett's test (** $p < 0.01$; *** $p < 0.001$; **** $p < 0.0001$).

The biological oxidative stress generation ability of the [AuCl(HL)] compounds on the intact parasites was confirmed. It can be concluded that the complexes would maintain the mechanisms of action of the 5-nitrofuryl pharmacophore.

Globally, the results of this work show that the inclusion of the Au(I) metal center does not have significant effects on the nitro anion radical generation of the thiosemicarbazone ligands. However, the presence of this metal ion means that the electron is preferably more localized in the nitro group than in the rest of the molecule. This behavior could be directly related to the antiparasitic activity shown by the complexes, as a correlation between the biological activity and their ability to generate ROS was observed. Compounds 2 and 3

were the most active gold compounds, and they produced a higher amount of ROS on *T. cruzi* parasites.

The anti-chagasic mechanism of action of the [AuCl(HL)] compounds is related to the damage by oxidative stress on *T. cruzi* parasites. However, their biological activity could also be associated with other mechanisms of action or with the interaction with biological targets. Studies recently performed have confirmed that [AuCl(HL)] compounds have a high interaction with DNA [18].

3. Materials and Methods

The [AuCl(HL)] (1–4) compounds studied in this work had been previously synthesized and fully characterized in solid state and solution [18].

3.1. Theoretical Calculations

Avogadro software (1.2.0n) [29] with the MMFF94 force field was utilized to perform a conformational search. The minimum energy conformation was obtained and then a geometry optimization was conducted using ORCA 5.0.4 [30]. SMD solvation model [31] with DMSO as the solvent was used to replicate the experimental conditions. All optimizations were carried out using the wB97XD functional with def2-TZVP basis set [32]. ECPs for the Au atom were performed [33–35].

The NBO analysis provides an accurate Lewis structure picture of the compounds using the highest percentage of orbital electron density representation [36–38]. This tool allows us to understand the intra and/or intermolecular interactions that occur between filled and virtual orbitals. Moreover, it gives information regarding charge density changes between atoms, which act as donors and/or acceptors with respect to a single molecule or different molecules interacting with each other. The relationship between donor (i) and acceptor (j) corresponds to the stabilization energy $E(2)$, which is estimated as:

$$E(2) = \Delta E_{ij} = q_i \frac{F(i,j)^2}{E_j - E_i}$$

where q_i is the donor orbital occupancy; E_i and E_j are diagonal elements, and $F(i,j)$ is the off-diagonal NBO Fock matrix element. A large $E(2)$ value corresponds to a stronger interaction between donor and electron acceptor atoms, which means a stronger donating tendency from donor to electron acceptor and consequently, a greater extension of the conjugation in the whole system, resulting in a stabilization of the system. All calculations were carried out using the NBO program.

3.2. Electrochemical Studies

The electrochemical behavior of the [AuCl(HL)] compounds was studied by cyclic voltammetry experiments recorded using a Methrom 797 VA. A standard electrochemical cell of three electrodes of 10 mL volume was used. The reduction process was studied employing a hanging drop mercury electrode (HDME) as working electrode, an Ag/AgCl electrode as a reference electrode, and a platinum wire as counter electrode. Measurements were performed at room temperature in 1 mM DMSO solutions of each gold complex, using tetrabutyl ammonium perchlorate (TBAP, 0.1 M) as supporting electrolyte. Solutions were deoxygenated via purging with nitrogen for 15 min prior to the measurements. A continuous gas stream was passed over the solutions between measurements.

3.3. ESR Spectroscopy

ESR spectra were recorded in the X band (9.85 GHz) using a Bruker ECS 106 spectrometer with a rectangular cavity and 50 kHz field modulation. The nitro anion radicals were generated by electrolytic reduction in situ, applying a potential corresponding to couple II obtained from the voltammetry studies. A platinum wire as working electrode and tetrabutyl ammonium perchlorate (TBAP, 0.1 M) as supporting electrolyte were used.

The compounds were dissolved in DMSO at room temperature and the solutions were deoxygenated via purging with nitrogen. Simulations of the experimental spectra were performed using the WINEPR-SimFonia 1.25 software. The hyperfine splitting constants were estimated to be accurate within 0.05 G.

The ESR parameters calculations of all gold compounds have also been obtained from the optimized structure using ORCA 5.0.4. Calculations of g and the isotropic part of hyperfine coupling constants were determined with the functional w97X with Def2-TZVP basis set. SMD solvent model was employed to describe the experimental conditions of the experimental data using DMSO as solvent.

3.4. Lipophilicity

Reversed-phase thin layer chromatography (TLC) experiments were performed on precoated TLC plates silica gel 60 RP-18 F254s using DMSO:PBS (80:20 *v/v*) as mobile phase (PBS: 10 mM Na₂HPO₄; 1.8 mM KH₂PO₄; 137 mM NaCl; 2.7 mM KCl; pH = 7.4). Stock solutions of the complexes and ligands were prepared in pure acetone (Aldrich) prior to use. The plates were developed in a closed chromatographic tank and dried, and the spots were located under UV light at 254 nm. The R_f values were averaged from three determinations, and converted to R_M via the relationship: $R_M = \log_{10}[(1/R_f) - 1]$ [12].

3.5. Biological Studies

3.5.1. Viability on *T. cruzi* (Dm28c) Trypomastigotes

Vero cells (CCL-81TM ATCC[®]) were infected with *Trypanosoma cruzi* metacyclic trypomastigotes from 15 days old. Subsequently, the trypomastigotes parasites harvested from this culture were used to infect further Vero cell cultures at a multiplicity of infection (MOI) of 10. These trypomastigote-infected Vero cell cultures were incubated at 37 °C in humidified air and 5% CO₂ for 72–96 h. After this time, trypomastigotes were harvested from the culture media, and then culture media were collected and centrifuged at 500 × g for 5 min (25 °C) to eliminate cellular detritus. The supernatant was then centrifuged at 4000 × g for 10 min (4 °C). The trypomastigote-containing pellets were resuspended in RPMI (without phenol red) media supplemented with 5% inactivated fetal bovine serum (FBSi) and penicillin (50 UI/mL)–streptomycin (50 µg/mL) at a final density of 1×10^7 parasites/mL. 2.2×10^8 trypomastigotes are equivalent to 1 mg of protein or 12 mg of wet weight. Viability assays were performed by using the MTT (3-(4,5-dimethylthiazol-2-yl)-2,5-diphenyl tetrazolium bromide) reduction method as previously described [39,40]. Briefly, 3×10^6 trypomastigotes were incubated in RPMI (without phenol red) culture medium with 5% FBSi at 37 °C for 24 h with and without the compounds under study at different concentrations, and Nifurtimox 10 µM as positive control. The compounds were dissolved in DMSO and diluted in culture media or PBS (0.1% DMSO) for biological experiments. An aliquot of the parasites suspensions was extracted, and it was incubated in a flat-bottom 96-well plate with MTT 0.5 mg/mL and phenazine 0.22 µg/mL at 37 °C for 3 h, and then, solubilized with 10% sodium dodecyl sulfate 0.01 N HCl and incubated overnight. Formazan formation was measured at 570 nm in a multiwell reader Varioskan Flash Multimode (Thermo Fisher[®], Santiago, Chile). Untreated parasites were used as negative controls (100% of cell viability). Finally, IC₅₀ values (concentration at which 50% of cell viability is inhibited) were determined by nonlinear regression with variable slope (four parameters) of viability versus log(concentration), by GraphPad8[®] software (version 8.0), for 4 independent experiments. The results are presented as the average of IC₅₀ with its standard deviation.

3.5.2. Cytotoxicity on Endothelial Mammalian Cells

The endothelial cell line EA.hy926 (a somatic hybrid cell with endothelial morphology) was maintained in Dulbecco's Modified Eagle's Medium (DMEM, Gibco[®], Santiago, Chile, high glucose and without phenol red), supplemented with 10% FBSi and penicillin (50 UI/mL)–streptomycin (50 µg/mL). Cells were maintained as a monolayer culture in

tissue culture flasks (Thermo Scientific Nunc™) in an incubator at 37 °C in a humidified atmosphere composed of 5% CO₂. A total of 5×10^4 cells were incubated per each well in a flat-bottom 96-well plate. After 24 h, the culture media was extracted and washed with PBS and then each compound concentration dissolved in culture media was added. Viability assays were performed using the MTT reduction method as previously described for *T. cruzi* trypanomastigote assay (see above) but without phenazine.

3.6. Insight into the Mechanism of Action

3.6.1. Generation of Free Radical Species in *T. cruzi*

The free radical production capacity of the gold(I) compounds was assessed in the *Trypanosoma cruzi* parasites with ESR spin trapping using DMPO (5,5-dimethyl-1-pyrroline-N-oxide) as spin trap. Each tested compound was dissolved in DMSO (spectroscopy grade, approximately 1 mM) and the solution was added to a mixture containing the trypanomastigote form of *T. cruzi* (Dm28 strain; 12 mg/mL), NADPH 1 mM, and DMPO 100 mM. The mixture was transferred to a 100 µL capillary. ESR spectra were recorded using an X-band Bruker ECS 106 spectrometer (9.85 GHz) with a rectangular cavity and 50 kHz field modulation. All the spectra were registered in the same scale, after 50 scans. The ESR spectra were simulated using WINEPR-SimFonia 1.25 software.

3.6.2. Intraparasitic Reactive Oxygen Species (ROS)

To study the generation of reactive oxygen species in trypanomastigotes of *T. cruzi* Dm28c after treatment with gold(I) compounds, the probe 2',7'-dihydrodichlorofluorescein diacetate (DCFH₂-DA) was used. Cell suspensions with 1×10^7 parasites/mL were used, which were incubated in 96-well plates with a PBS solution of 20 µM DCFH₂-DA for 15 min at 37 °C and 5% CO₂. The loaded parasites were centrifuged and washed with PBS in duplicate. Gold(I) compounds were added to the loaded parasites at a concentration of 10 µM, using 10 µM Nifurtimox as a positive control and untreated parasites as a negative control. Fluorescence ($\lambda_{\text{ex.}} = 488 \text{ nm}$; $\lambda_{\text{em.}} = 528 \text{ nm}$) was recorded for 60 min and every 1 min. The area under the curve of relative fluorescence versus time was calculated using OriginPro8.5® software (Version 10.0) and normalized versus the negative control. The results of three independent experiments (N = 3) are presented as the average of the area ratio of increased fluorescence with respect to the negative control, with its standard deviation. For each treatment, a one-way analysis of variance (ANOVA) with subsequent Dunnett's test using OriginPro 8.5® software.

4. Conclusions

The chemical structure of four gold compounds, [AuCl(HL)], that include 5-nitrofuryl-containing thiosemicarbazones as bioactive ligands were theoretically calculated. All compounds showed identical structures, with the metal ion located in a linear coordination environment and the thiosemicarbazones acting as monodentate ligands.

Natural Bond Orbital (NBO) results showed that the compounds present a large zone of electronic delocalization centered on the nitro anion radical. Cyclic voltammetry studies confirmed that the compounds can be reduced to generate the nitro anion radical (NO₂^{•-}). An almost negligible effect on the nitro moiety reduction potential was observed as a consequence of Au(I) complexation. The presence of this reduction process is biologically relevant since it would favor the toxic radical oxygen species (ROS) generation in *Trypanosoma cruzi*. Electron Spin Resonance (ESR) studies allowed the determination of the hyperfine coupling constants for the gold compounds and ORCA calculations allowed their spin densities to be determined, which confirmed the existence of a great localization of the unpaired electron in the nitrogen atom of the nitro group.

The compounds were active against the bloodstream form of *T. cruzi* with IC₅₀ values in the micromolar range. Complexes 2 and 3 were the most active compounds and showed an enhancement in antiparasitic activity compared with their respective bioactive ligands. The compounds showed moderate selectivity towards the parasites concerning the selected

mammalian cell model. Regarding the probable mechanism of action, the compounds were capable of producing free radical species in the intact parasites. Using spin trapping with ESR and fluorescence measurements it was possible to identify, characterize, and quantify the reactive oxygen species generated within the parasites after the treatment with gold(I) compounds.

Globally, these results show a relationship between the ROS generation ability and the antiparasitic activity of the [AuCl(HL)] compounds, hence the potential oxidative stress mechanism against *T. cruzi* could be confirmed. Gold(I) compounds containing thiosemicarbazones are promising antiparasitic compounds that deserve further studies in the search for prospective broad-spectrum drugs.

Supplementary Materials: The following supporting information can be downloaded at: <https://www.mdpi.com/article/10.3390/inorganics12050133/s1>, Table S1: Natural Bond Orbital (NBO) results for [AuCl(HL2)] (2) compound; Table S2: Natural Bond Orbital (NBO) results for [AuCl(HL3)] (3) compound; Table S3: Natural Bond Orbital (NBO) results for [AuCl(HL)] (4) compound; Figure S1: Natural Bond Orbital (NBO) selected bond for [AuCl(HL1)] (1) compound; Figure S2: Natural Bond Orbital (NBO) selected bond for [AuCl(HL2)] (2) compound; Figure S3: Natural Bond Orbital (NBO) selected bond for [AuCl(HL3)] (3) compound; Figure S4: Natural Bond Orbital (NBO) selected bond for [AuCl(HL4)] (4) compound; Figure S5: Spin density calculated for [AuCl(HL2)] (2) compound; Figure S6: Spin density calculated for [AuCl(HL3)] (3) compound; Figure S7: Spin density calculated for [AuCl(HL3)] (3) compound; Table S4: Spin density calculated by ORCA for [AuCl(HL)] compounds; Figure S8: Correlation between the anti-*T. cruzi* activity and the hyperfine splitting constant on the nitrogen atom (N6) and R_M values of the [AuCl(HL)] compounds; Figure S9: Rate of increase in areas of fluorescence spectra concerning the compound 3.

Author Contributions: Experimental work, J.Ó.-R. Theoretical calculations, P.R. and G.B.-G.; Biological studies, J.O.-C. and A.L.; investigation, D.G. and L.O.; supervision, C.O.A. and U.K.; writing—review and editing, E.R.-A. All authors have read and agreed to the published version of the manuscript.

Funding: This research was funded by ANID/FONDECYT/POSTDOC project N°3200449 (E.R.A) and by ANID/FONDECYT regular project N°1230644 (C.O.A).

Data Availability Statement: The information provided in this research is accessible in both the manuscript and its Supplementary Materials.

Conflicts of Interest: The authors declare no conflicts of interest.

References

1. Available online: www.who.int/health-topics/neglected-tropical-diseases#tab=tab_1 (accessed on 5 April 2024).
2. Available online: [https://www.who.int/news-room/fact-sheets/detail/chagas-disease-\(american-trypansomiasis\)](https://www.who.int/news-room/fact-sheets/detail/chagas-disease-(american-trypansomiasis)) (accessed on 5 April 2024).
3. Bermudez, J.; Davies, C.; Simonazzi, A.; Pablo Real, J.; Palma, S. Current Drug Therapy and Pharmaceutical Challenges for Chagas Disease. *Acta Trop.* **2016**, *156*, 1–16. [[CrossRef](#)] [[PubMed](#)]
4. Scarim, C.B.; Jornada, D.H.; Chelucci, R.C.; de Almeida, L.; dos Santos, J.L.; Chung, M.C. Current Advances in Drug Discovery for Chagas Disease. *Eur. J. Med. Chem.* **2018**, *155*, 824–838. [[CrossRef](#)]
5. Francisco, A.F.; Jayawardhana, S.; Olmo, F.; Lewis, M.D.; Wilkinson, S.R.; Taylor, M.C.; Kelly, J.M. Challenges in Chagas Disease Drug Development. *Molecules* **2020**, *25*, 2799. [[CrossRef](#)] [[PubMed](#)]
6. Brindha, J.; Balamurali, M.M.; Chanda, K. An Overview on the Therapeutics of Neglected Infectious Diseases—Leishmaniasis and Chagas Diseases. *Front. Chem.* **2021**, *9*, 622286.
7. Brown, R.W.; Hyland, C.J.T. Medicinal Organometallic Chemistry—An Emerging Strategy for the Treatment of Neglected Tropical Diseases. *MedChemComm* **2015**, *6*, 1230–1243. [[CrossRef](#)]
8. Gambino, D.; Otero, L. Design of Prospective Antiparasitic Metal-Based Compounds Including Selected Organometallic Cores. *Inorg. Chim. Acta* **2018**, *472*, 58–75. [[CrossRef](#)]
9. Ong, Y.C.; Roy, S.; Andrews, P.C.; Gasser, G. Metal Compounds against Neglected Tropical Diseases. *Chem. Rev.* **2019**, *119*, 730–796. [[CrossRef](#)]
10. Aguirre, G.; Boiani, L.; Cerecetto, H.; Fernández, M.; González, M.; Denicola, A.; Otero, L.; Gambino, D.; Rigol, C.; Olea-Azar, C.; et al. In Vitro Activity and Mechanism of Action against the Protozoan Parasite *Trypanosoma cruzi* of 5-Nitrofuryl Containing Thiosemicarbazones. *Bioorg. Med. Chem.* **2004**, *12*, 4885–4893. [[CrossRef](#)]

11. Gambino, D.; Otero, L. Facing Diseases Caused by Trypanosomatid Parasites: Rational Design of Pd and Pt Complexes with Bioactive Ligands. *Front. Chem.* **2022**, *9*, 816266. [[CrossRef](#)]
12. Rodríguez Arce, E.; Putzu, E.; Lapiere, M.; Maya, J.D.; Olea Azar, C.; Echeverría, G.A.; Piro, O.E.; Medeiros, A.; Sardi, F.; Comini, M.; et al. New Heterobimetallic Ferrocenyl Derivatives Are Promising Antitrypanosomal Agents. *Dalton Trans.* **2019**, *48*, 7644–7658. [[CrossRef](#)]
13. Glišić, B.Đ.; Djuran, M.I. Gold Complexes as Antimicrobial Agents: An Overview of Different Biological Activities in Relation to the Oxidation State of the Gold Ion and the Ligand Structure. *Dalton Trans.* **2014**, *43*, 5950–5969. [[CrossRef](#)] [[PubMed](#)]
14. Proetto, M.T.; Alexander, K.; Melaimi, M.; Bertrand, G.; Gianneschi, N.C. Cyclic (Alkyl)(Amino)Carbene (CAAC) Gold(I) Complexes as Chemotherapeutic Agents. *Chem.—Eur. J.* **2021**, *27*, 3772–3778. [[CrossRef](#)] [[PubMed](#)]
15. Navarro, M.; Cisneros-Fajardo, E.J.; Lehmann, T.; Sánchez-Delgado, R.A.; Atencio, R.; Silva, P.; Lira, R.; Urbina, J.A. Toward a Novel Metal-Based Chemotherapy against Tropical Diseases. Synthesis and Characterization of New Copper(II) and Gold(I) Clotrimazole and Ketoconazole Complexes and Evaluation of Their Activity against *Trypanosoma cruzi*. *Inorg. Chem.* **2001**, *40*, 6879–6884. [[CrossRef](#)] [[PubMed](#)]
16. Vieites, M.; Smircich, P.; Guggeri, L.; Marchán, E.; Gómez-Barrio, A.; Navarro, M.; Garat, B.; Gambino, D. Synthesis and Characterization of a Pyridine-2-Thiol *N*-Oxide Gold(I) Complex with Potent Antiproliferative Effect against *Trypanosoma cruzi* and *Leishmania* Sp. Insight into Its Mechanism of Action. *J. Inorg. Biochem.* **2009**, *103*, 1300–1306. [[CrossRef](#)] [[PubMed](#)]
17. Massai, L.; Messori, L.; Micale, N.; Schirmeister, T.; Maes, L.; Fregona, D.; Cinellu, M.A.; Gabbiani, C. Gold Compounds as Cysteine Protease Inhibitors: Perspectives for Pharmaceutical Application as Antiparasitic Agents. *BioMetals* **2017**, *30*, 313–320. [[CrossRef](#)] [[PubMed](#)]
18. Rodríguez-Arce, E.; Gavrilov, E.; Alvite, X.; Nayeem, N.; León, I.E.; Neary, M.C.; Otero, L.; Gambino, D.; Olea Azar, C.; Contel, M. 5-Nitrofuryl-Containing Thiosemicarbazone Gold(I) Compounds: Synthesis, Stability Studies, and Anticancer Activity. *ChemPlusChem* **2023**, *88*, e202300115. [[CrossRef](#)] [[PubMed](#)]
19. Dorosti, Z.; Yousefi, M.; Sharafi, S.M.; Darani, H.Y. Mutual Action of Anticancer and Antiparasitic Drugs: Are There Any Shared Targets? *Future Oncol.* **2014**, *10*, 2529–2539. [[CrossRef](#)]
20. Sullivan, J.A.; Tong, J.L.; Wong, M.; Kumar, A.; Sarkar, H.; Ali, S.; Hussein, I.; Zaman, I.; Meredith, E.L.; Helsby, N.A.; et al. Unravelling the Role of SNM1 in the DNA Repair System of *Trypanosoma brucei*. *Mol. Microbiol.* **2015**, *96*, 827–838. [[CrossRef](#)] [[PubMed](#)]
21. Perez, M.J.; Fuertes, A.M.; Nguewa, A.P.; Castilla, J.; Alonso, C. Anticancer Compounds as Leishmanicidal Drugs: Challenges in Chemotherapy and Future Perspectives. *Curr. Med. Chem.* **2008**, *15*, 433–439. [[CrossRef](#)]
22. Guerini, A.E.; Triggiani, L.; Maddalo, M.; Bonù, M.L.; Frassine, F.; Baiguini, A.; Alghisi, A.; Tomasini, D.; Borghetti, P.; Pasinetti, N.; et al. Mebendazole as a Candidate for Drug Repurposing in Oncology: An Extensive Review of Current Literature. *Cancers* **2019**, *11*, 1284. [[CrossRef](#)]
23. Son, D.-S.; Lee, E.-S.; Adunyah, S.E. The Antitumor Potentials of Benzimidazole Anthelmintics as Repurposing Drugs. *Immune Netw.* **2020**, *20*, e29. [[CrossRef](#)] [[PubMed](#)]
24. Otero, L.; Vieites, M.; Boiani, L.; Denicola, A.; Rigol, C.; Opazo, L.; Olea-Azar, C.; Maya, J.D.; Morello, A.; Krauth-Siegel, R.L.; et al. Novel Antitrypanosomal Agents Based on Palladium Nitrofurylthiosemicarbazone Complexes: DNA and Redox Metabolism as Potential Therapeutic Targets. *J. Med. Chem.* **2006**, *49*, 3322–3331. [[CrossRef](#)] [[PubMed](#)]
25. Rigol, C.; Olea-Azar, C.; Mendizábal, F.; Otero, L.; Gambino, D.; González, M.; Cerecetto, H. Electrochemical and ESR Study of 5-Nitrofuryl-Containing Thiosemicarbazones Antiprotozoal Drugs. *Spectrochim. Acta A Mol. Biomol. Spectrosc.* **2005**, *61*, 2933–2938. [[CrossRef](#)]
26. Pagano, M.; Demoro, B.; Toloza, J.; Boiani, L.; González, M.; Cerecetto, H.; Olea-Azar, C.; Norambuena, E.; Gambino, D.; Otero, L. Effect of Ruthenium Complexation on Trypanocidal Activity of 5-Nitrofuryl Containing Thiosemicarbazones. *Eur. J. Med. Chem.* **2009**, *44*, 4937–4943. [[CrossRef](#)] [[PubMed](#)]
27. Vieites, M.; Otero, L.; Santos, D.; Toloza, J.; Figueroa, R.; Norambuena, E.; Olea-Azar, C.; Aguirre, G.; Cerecetto, H.; González, M.; et al. Platinum(II) Metal Complexes as Potential Anti-*Trypanosoma cruzi* Agents. *J. Inorg. Biochem.* **2008**, *102*, 1033–1043. [[CrossRef](#)] [[PubMed](#)]
28. Makino, K.; Hagiwara, T.; Murakami, A. A Mini Review: Fundamental Aspects of Spin Trapping with DMPO. *Int. J. Radiat. Appl. Instrum. Part C Radiat. Phys. Chem.* **1991**, *37*, 657–665. [[CrossRef](#)]
29. Hanwell, M.D.; Curtis, D.E.; Lonie, D.C.; Vandermeersch, T.; Zurek, E.; Hutchison, G.R. Avogadro: An Advanced Semantic Chemical Editor, Visualization, and Analysis Platform. *J. Cheminform.* **2012**, *4*, 17. [[CrossRef](#)] [[PubMed](#)]
30. Neese, F. The ORCA Program System. *WIREs Comput. Mol. Sci.* **2012**, *2*, 73–78. [[CrossRef](#)]
31. Marenich, A.V.; Cramer, C.J.; Truhlar, D.G. Universal Solvation Model Based on Solute Electron Density and on a Continuum Model of the Solvent Defined by the Bulk Dielectric Constant and Atomic Surface Tensions. *J. Phys. Chem. B* **2009**, *113*, 6378–6396. [[CrossRef](#)]
32. Weigend, F.; Ahlrichs, R. Balanced Basis Sets of Split Valence, Triple Zeta Valence and Quadruple Zeta Valence Quality for H to Rn: Design and Assessment of Accuracy. *Phys. Chem. Chem. Phys.* **2005**, *7*, 3297–3305. [[CrossRef](#)]
33. Dolg, M.; Stoll, H.; Preuss, H. Energy-adjusted Ab Initio Pseudopotentials for the Rare Earth Elements. *J. Chem. Phys.* **1989**, *90*, 1730–1734. [[CrossRef](#)]

34. Andrae, D.; Häußermann, U.; Dolg, M.; Stoll, H.; Preuß, H. Energy-Adjusted ab Initio Pseudopotentials for the Second and Third Row Transition Elements. *Theor. Chim. Acta* **1990**, *77*, 123–141. [[CrossRef](#)]
35. Peterson, K.A.; Figgen, D.; Goll, E.; Stoll, H.; Dolg, M. Systematically Convergent Basis Sets with Relativistic Pseudopotentials. II. Small-Core Pseudopotentials and Correlation Consistent Basis Sets for the Post-d Group 16–18 Elements. *J. Chem. Phys.* **2003**, *119*, 11113–11123. [[CrossRef](#)]
36. Reed, A.E.; Curtiss, L.A.; Weinhold, F. Intermolecular Interactions from a Natural Bond Orbital, Donor-Acceptor Viewpoint. *Chem. Rev.* **1988**, *88*, 899–926. [[CrossRef](#)]
37. Foster, J.P.; Weinhold, F. Natural Hybrid Orbitals. *J. Am. Chem. Soc.* **1980**, *102*, 7211–7218. [[CrossRef](#)]
38. Zapata-Torres, G.; Fierro, A.; Barriga-González, G.; Salgado, J.C.; Celis-Barros, C. Revealing Monoamine Oxidase B Catalytic Mechanisms by Means of the Quantum Chemical Cluster Approach. *J. Chem. Inf. Model.* **2015**, *55*, 1349–1360. [[CrossRef](#)] [[PubMed](#)]
39. Muelas-Serrano, S.; Nogal-Ruiz, J.J.; Gómez-Barrio, A. Setting of a Colorimetric Method to Determine the Viability of *Trypanosoma cruzi* Epimastigotes. *Parasitol. Res.* **2000**, *86*, 999–1002. [[CrossRef](#)]
40. Faundez, M.; Pino, L.; Letelier, P.; Ortiz, C.; López, R.; Seguel, C.; Ferreira, J.; Pavani, M.; Morello, A.; Maya, J.D. Buthionine Sulfoximine Increases the Toxicity of Nifurtimox and Benznidazole to *Trypanosoma cruzi*. *Antimicrob. Agents Chemother.* **2005**, *49*, 126–130. [[CrossRef](#)]

Disclaimer/Publisher's Note: The statements, opinions and data contained in all publications are solely those of the individual author(s) and contributor(s) and not of MDPI and/or the editor(s). MDPI and/or the editor(s) disclaim responsibility for any injury to people or property resulting from any ideas, methods, instructions or products referred to in the content.